The synergy of microplastics with the heavy metal zinc has resulted in reducing the toxic effects of zinc on lentil (*Lens culinaris*) seed germination and seedling growth

Y. Sanath K. De Silva [a,b,***], Uma Maheswari Rajagopalan [c,**], Hirofumi Kadono [a,*], Danyang Li [a]

[a] *Graduate School of Science and Engineering, Saitama University, 255 Shimo-okubo, Sakura-ku, Saitama-shi, Saitama, 338-8570, Japan*
[b] *Department of Mechanical and Manufacturing Engineering, Faculty of Engineering, University of Ruhuna, Hapugala, Galle, 80000, Sri Lanka*
[c] *Department of Mechanical Engineering, Shibaura Institute of Technology, 3-7-5 Toyosu, Koto City, Tokyo, 135-8548, Japan*

ARTICLE INFO

ABSTRACT

There is growing recognition of the impact of the rising presence of microplastics (MPs) on terrestrial plant growth and, in general, the terrestrial ecosystem. Simultaneously, there is growing heavy metal accumulation in agricultural lands at an astonishing rate owing to the overwhelming use of chemical fertilizers, herbicides, and weedicides. Thus, there is a need to investigate the synergetic effect of MPs along with heavy metals on the inducing combined toxicity. This study investigates effects at smaller exposure periods of a few hours using a novel optical imaging technique, Biospeckle Coherence Tomography. Biospeckle Optical Coherence Tomography (bOCT) is a novel optical imaging technique that we successfully demonstrated earlier in visualizing the internal activity of plants. Previous studies of authors using the bOCT technique have demonstrated its potential in the independent application of polyethylene microplastic (PEMPs) as well as zinc within 6 h after their treatments. The strong inhibitory effect of 100 mg L^{-1}, Zn, and PEMPs alone on the germination of *Lens culinaris* could be visualized with bOCT. The current study demonstrated that against expectation, combined effects of Zn toxicity were reduced when combined with MPs. This is suggested due to the significant reduction of Zn uptake by the seedlings through the interaction of Zn and MPs in an aqueous solution. Mass-spectrometry results also indicate a reduced intake of Zn. Our findings suggest that PEMPs could be able to reduce the over-availability of Zn, thus mitigating the Zn toxicity on lentils.

1. Introduction

The mass production of plastic has begun since 1940 while providing benefits for humans and emerging problems for the world [1]. Recently, special attention has been paid to micro (5 mm - 100 nm) and nano (100 nm–1 nm) sized plastics owing to the growing health

---

effects on humans and the adverse effect on plant growth. However, microplastics (MPs) are categorized as primary or secondary depending on how they form [2]. When larger plastic particles break apart due to natural factors like biodegradation, mechanical degradation, and physical stress, secondary MPs are created. The primary MPs are made with a particle size of less than 5 mm [3].

Initially, less attention was paid to monitoring the impact of MPs on terrestrial ecosystems compared to the aquatic ecosystem. However, recently the attention has shifted toward the terrestrial environment because of rapid MP accumulation through plastic mulching, road dust, sewage sludge, atmospheric deposition, landfilling, etc. [4]. Accumulation of MPs in the terrestrial ecosystem can induce a potentially adverse impact on plant growth by inhibiting growth and seed germination. In the case of seeds, MPs play a role in the physical blockage of the pores that reduce uptake of water and nutrients [5,6]. Our previous studies employed bOCT in the investigation of the individual effects of PEMPs on lentils and demonstrated the dose-dependent adverse effects under different concentrations of MPs exposure (10, 50, and 100 mg L^{-1}) [7,8].

In addition to MPs, there is also an increase in the accumulation of heavy metals on agricultural soil as a result of the widespread usage of chemical fertilizers, pesticides, mining, etc. This in turn affects the seed germination and plant growth [9]. One such heavy metal Zn which is also, in smaller amounts, a crucial micronutrient for plant development. Zn acts as a catalytic cofactor and promotes the activity of numerous enzymes and metabolic processes. However, an excess Zn (>50 mg L^{-1}) becomes toxic, significantly reducing the seed germination and seedling growth [10–12]. We demonstrated earlier both the micronutrient (5, 10 mg L^{-1}) and toxic effects of Zn concentrations (100 mg L^{-1}) on seed germination using bOCT. The results imply a positive effect for 5 mg L^{-1} and 10 mg L^{-1}, whereas 100 mg L^{-1} Zn exhibits a strong toxic effect on lentils [13].

Because of the possibility of the of simultaneous availability of MPs and Zn, there could be combined effects and a few studies reported the adsorption ability of heavy metals such as Cu^{2+} and Zn^{2+} on microplastics [14]. MPs have properties such as large specific surface area, surface functional groups and ageing, making them excellent heavy metal carriers that can easily be transported and migrated into different environmental media [15]. The adsorption of metals onto MPs can be explained by a variety of best-fit isotherms. The Langmuir model is the most popular and practical isotherms model for the investigation of heavy metal adsorption on MPs, which indicates the primary mechanism of chemisorption [16]. The chemical properties of heavy metals, the nature and features of polymers, and environmental conditions like pH, salinity, and variations in background pollutant concentrations all impact the adsorption process [10].

Moreover, the adsorption ability of PE, PS and PVC follow the order of PS (128.5 μg/g) < PE (416.7 μg/g) < PVC (483.1 μg/g), emphasizing the heavy metal adsorption ability of PEMPs [17]. Therefore, the co-existence of MPs and heavy metal could mitigate the magnitude of heavy metal toxicity in agriculture. According to the literature, there are different methods adopted to reduce heavy metal toxicity in agricultural farmlands since heavy metal accumulation is one of the major agronomic challenges that has seriously threatened food safety. Especially, a few microbes, particularly those in the group of rhizobacteria that promote plant growth (PGPR) with high metal tolerating ability and exhibiting unique plant growth promoting potentials [18,19]. Moreover, there are some attempts to realize the significance of chemo-mechanical coupling on the precipitation kinetics [20]. A few studies have demonstrated the combined effect of metal-microplastics on plant growth [21–24]. The results of those studies imply the reduction of heavy metal toxicity and bioavailability of heavy metal when combined with microplastics. However, existing knowledge regarding the synergic effects of microplastic on plant growth is limited, and more research studies are needed to estimate and manage the risks involved.

There is a high possibility of accumulating PEMPs in agricultural lands through plastic mulching, inducing an adverse effect on seed germination and plant growth [25]. Urbina et al. [5] reported the retarded growth of hydroponic maize plants owing to the accumulation of PEMPs on the root due to the reduced water and nutrient uptake. Moreover, PEMPs can adsorb various environmental pollutants inducing combined toxicity [26,27].

Lentils are a widely grown legume crop and popular because of its ease of cultivation. It is commercially significant due to its high protein, fiber, low calories, essential amino acids, fatty acids, and trace minerals [28]. Due to its enhanced consumption, the demand for lentils is anticipated to rise from 6.3 million tons in 2018 to 8.4 million tons in 2024 globally. All the above factors make lentil species a model plant to observe the impact of various environmental stresses on seed germination [8,29].

Existing research report on the combined effect of MPs and heavy metals is restricted to seedling growth, i.e., after the germination occurred, and not on the germination process itself [21]. Moreover, numerous research works have explored the individual and synergic effects of MPs and heavy metals on plants and reported different effects particularly after the germination occurred [30,31]. Most of the procedures employed in previous works are invasive and sample preparation is time-consuming. A significant effect was observed after considerable exposure time. However, so far, no studies have been presented which can observe the effect at an early stage before the germination in the case of seed. Therefore, in this study, we focus on visualizing the changes in internal biological activities before germination using a technique called biospeckle Optical Coherence Tomography (OCT).

OCT is a non-invasive technique capable of mapping the internal structure of biological tissues in 2D or 3D in vivo [32]. Because the technique is based interferometery, it is highly sensitive and has a wide dynamic range and has been successfully applied as a clinical tool in ophthalmology to visualize the retinal structures and in biomedical fields [33]. There exists a few reports on its application to plant and agriculture fields [34,35]. The focus of OCT related works has been more on the structure itself because of its ability to observe only the internal structures. However, in our case, we focused on the temporal variation of the internal structures. Such temporal variation in the structures would result in the formation of dynamic speckles that appear as noise in the OCT structure images and are spatially averaged out. In our case, we intentionally used these speckles and developed a method, biospeckl OCT, to investigate the temporal variation. In bOCT, the changes with respect to time were observed as a bOCT contrast or as a fluctuation. bOCT has been successfully employed to monitor biological activities inside plants and has been demonstrated to investigate the effects of Ozone on leaves [36,37], and growth hormone, gibberellic acid (GA3) [38]. bOCT has also been used successfully to study seed germination under the impact of environmental conditions [39] on such as, Zn [13], PEMPs alone on lentil seeds [7], Acid Mine Drainage's (AMD)

[40,41] and effect of AMD on monocot and dicot seed germination [42]. In the present study, bOCT was used to assess the individual toxic effect of PEMPs and Zn and their synergic effects followed by comparison with the conventional measures.

2. Materials and methods

2.1. Preparation of particles and chemical reagents

PEMPs in dry powder form were bought from Cospheric LLC (Santa Barbara, California 93160, USA) with specified particle sizes of 740–4990 nm. To overcome the hydrophobic properties of the particles and obtain proper dispersing capabilities, a non-ionic, biocompatible surfactant emulsion solution of 0.05 % tween 80 was created. Based on a previous study by authors, PEMPs concentrations of 100 mg L^{-1} were prepared to provide maximum adverse effects [7]. The solutions were first vortexed for 1 min, then centrifuged for 5 min, and then sonicated at 28 °C for 10 min to achieve the high dispersity and uniformity of the emulsion. The procedure was repeated until all of the particles were evenly distributed and there were no PEMP clusters visible in the stock solutions.

Zinc nitrate hexahydrate (Zn $(NO_3)_2.6H_2O$) (99 % purity) was purchased from FUJIFILM Wako Pure Chemical Corporation (Osaka, Japan) and used as the Zn source. The concentrations of 100 mg L^{-1} Zn were prepared for the experiments to provide maximum adverse effects based on our previous study [13].
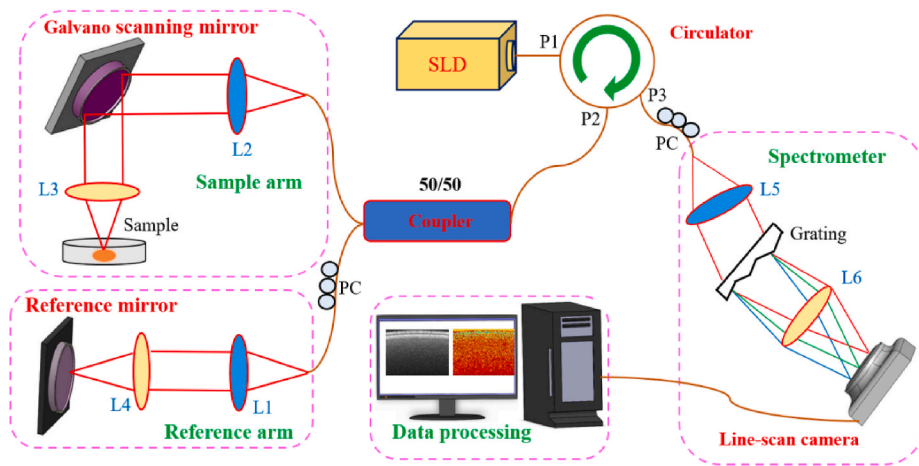
(a)
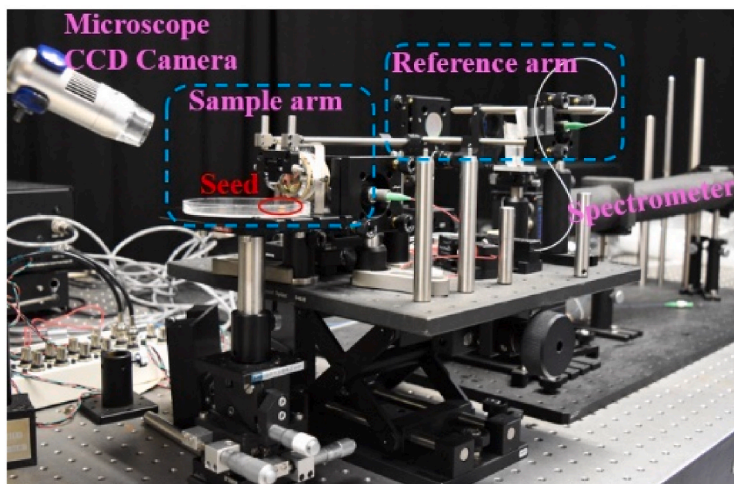
(b)

Fig. 1. An illustration of the experimental biospeckle Optical Coherence Tomography system and a picture of it with a sample seed lighted are shown in (a) and (b), respectively.

2.2. Seed breeding and treatments

To observe the individual and combined toxicity of MPs and Zn, four treatment groups were prepared, namely, control, 100 mg L^{-1} PEMPs, 100 mg L^{-1} Zn, 100 mg L^{-1} PEMPs and 100 mg L^{-1} Zn mixture. The lentil seeds were obtained from Greenfield Project Co., Ltd., a company that produces organic seeds, and they were stored in a dry area until usage. The chosen seeds, which weighed around 40 mg, underwent sterilization by being submerged in a 2.5 % H_2O_2 solution for 15 min. They were then thoroughly rinsed three times with distilled water to eliminate extra surfactant. For the OCT experiments, six seeds of lentils were placed in each Petri dish and kept inside a growth chamber (Conviron, Controlled Environmental Ltd, Canada) that was maintained at an air temperature of 25 °C/20 °C, a light intensity of 260–350 μmol m^{-2} s^{-1}/0 μmol m^{-2} s^{-1}, and relative humidity of 55–65 % following a 12 h/12 h cycle. The same seed breeding protocol was followed for conventional measurement experiments where 12 seeds were used for each treatment with the triplicate sample.

2.3. Optical coherent tomography (OCT) experimental setup and procedure

For brevity of the paper, a basic description of the system is given in this paper and details explanation of the experimental system and procedures could be found in detail [7,13]. A schematic diagram and a photo of the actual system are shown in Fig. 1 a and Fig. 1 b, respectively. The spectral interference obtained was first converted from wavelength to k-space and then, Fourier transformation was used to acquire the depth-resolved reflectivity profile of the sample. A total of 100 frames of 2048 (x) 512 (z) pixels were captured while the Galvano mirrors were scanning the probing beam at a rate of 10 frames per second. The acquired OCT structural images were analyzed to calculate the biospeckle contrast. Using Equations (1) and (2), the system's axial (z) and lateral (x) resolutions in plant tissue were calculated to be 6 μm and 22 μm, respectively.

$$\Delta z = \frac{2 \ln 2}{\pi\, n} \frac{\lambda_0{}^2}{\Delta \lambda}, \tag{1}$$

$$\Delta x = \frac{4 \lambda_0}{\pi} \left[\frac{f}{d} \right], \tag{2}$$

To mitigate the effect of moisture on the seed coat, the lentil seeds were adequately dried with paper towels before the OCT experiments were conducted. Six seeds were used for each treatment. The orientation and scanning position are important for the comparison of bOCT images. Therefore, special attention was paid to keeping the seed at the same orientation and scanning position for each scan. Due to its inherent curvature, the bottom surface area closest to the seeds' meridians makes the strongest contact with the liquid solution inside the Petri dish. Therefore, to ensure that OCT images of all the seeds were obtained from the same position, all the seeds were fixed and set in a proper orientation that would allow the center of the seeds to be progressively scanned.

2.4. Biospeckle contrast

The phenomenon known as "biospeckle" is caused when a biological object is exposed to coherent light, such as laser light, and the scattered light interferes [43]. Due to the scattering centers' constant motion, which includes cytoplasmic streaming, organelle movement, cell development, cell division, and biochemical reactions, a dynamic speckle pattern could be seen for biological objects. However, the intensity of the speckle pattern is constant over time for a static object.

In this research, the temporal variation of the collected OCT structural images was evaluated using a quantity called biospeckle contrast (γ), which is defined as the ratio of the standard deviation of the intensity to the mean value at each pixel along the temporal axis. The definition of this biospeckle comparison can be found in Eq. (3).

$$\gamma(x,y) = \frac{1}{< I_{OCT}(x,y) >} \left[\frac{1}{N} \sum_{j=1}^{N} \left\{ I_{OCT}(x,y;t_j) - \; < I_{OCT}(x,y) > \right\}^2 \right]^{\frac{1}{2}}, \tag{3}$$

$$< I_{OCT}(x,y) > \; = \frac{1}{N} \sum_{j=1}^{N} I_{OCT}(x,y;t_j),$$

where x and y stand for the coordinates of a single pixel, j for the scan number, and N for the total number of scans. The seeds' larger temporal fluctuation or speckle contrast indicates that they have undergone considerable alterations over time. As a result, the variations in speckle contrast magnitude may be a valuable indicator of the biological activity of seeds in the presence of outside agents.

2.5. Seed vigor observation

The Triphenyl Tetrazolium Chloride (TTC) test was used to assess lentil seed vigor after being exposed to different treatments. The TTC test is a commonly used invasive chemical method to distinguish metabolically active and inactive seeds. The test relies on the reduction of the colorless and water-soluble triphenyl tetrazolium chloride (TTC) to an insoluble red compound TPF (1,3,5 triphenylformazan) [44]. The viability of seeds that have failed to germinate could be accurately assessed by the TTC test. In the beginning, lentil seeds that were exposed to relevant treatments for 24 h were selected and appropriately dried before being soaked in 1 % TTC

solution for 3 h. The soaking in TTC solution was performed in dark conditions at a temperature of 30 °C. Finally, the reduction of TTC was extracted with ethyl acetate at 458 nm [45].

2.6. Seed germination and seedling growth

To compare the bOCT results with conventional measurements, seed germination and seedling growth parameters were measured. Germination rate and viability were used as the germination parameters, whereas root length, shoot length, and fresh and dry weight of seedlings were considered as the seedling growth parameters.

2.6.1. Seed germination

Lentil seeds often begin to germinate after 24 h of exposure. The seeds were deemed to have germinated when their radical extension measured roughly 2 mm [46]. The seeds were removed from the Petri dishes if fungus developed on the seed coat, indicating that they were dead seeds. In this study, seed germination was observed after 2 and 7 days of exposure, and the following germination requirements were determined.

$$Germination\ Viability(GV,\%) = \frac{N_g\ at\ day\ 2}{N_t} X\ 100\ \%, \tag{4}$$

$$Germination\ Rate(GR,\%) = \frac{N_g\ at\ day\ 7}{N_t} X\ 100\ \%, \tag{5}$$

where N_t is the total number of seeds utilized in the particular batch and N_g is the number of seeds that germinated on specific exposure days.

2.6.2. Growth of seedlings

After being exposed for 7 days, seedling development was noted. Six seedlings from each sample, control samples and samples subjected to PEMPs were selected, and they underwent five thorough cleanings with distilled water to get rid of unwelcome surfactants. Thereafter, seedlings' shoot and root lengths were measured at the root-shoot junction with the photographs of the seedlings samples using ImageJ software (NIH, USA).

Weighing was done on all of the removed roots and shoots individually through an analytical scale to observe the fresh weight of seedlings (AUX 320, UniBloc, Shimadzu, Japan). Afterwards, separated roots and shoots were placed in an oven (SOFW–450S, AS ONE, Japan) at 105 °C for 15 min, then at 70 °C until they reached a constant weight, which was then measured to determine their dry weight.

2.7. Quantification of Zn uptake

The Zn concentration of 7 d old lentil seedlings was quantified using Inductively Coupled Plasma – Atomic Emission Spectrometry, ICP-AES (PerkinElmer Optima 5300DV, Gen tech scientific, United States), with triplicate samples to compare with bOCT results. First, lentil seedlings were oven-dried to obtain a constant weight. Next, 0.2 g of dry sample from each treatment was weighed and digested by adding 2 ml of 1:1 HNO_3 acid solution. To make sure the complete reaction with HNO_3, the digestive fluid was warmed to 95 °C until it no longer produced any brown exhaust, the sample. After that, 0.4 ml of water, and 0.6 ml of 30 % H_2O_2 were added to the chilled sample and heated until the effervescence was negligible, or the overall appearance of the sample remained unchanged. The solution volume was lowered to around 1 ml after 2 h of heating at 95 °C without boiling. The digested sample was mixed with 2 ml concentrated HCl for the sample analysis, and it was then heated for 15 min at 95 °C. The Whatman filter paper was used to filter the digest. A 20 ml volumetric flask with a 20 ml set volume was used to collect the filtrate. ICP-AES was used to measure the Zn uptake from the treated samples.

2.8. Statistical analysis

The average and standard deviation of the mean are used to present the findings of each sample that was tested in triplicate. Using SPSS 16.0, one-way analysis of variance (ANOVA, p 0.05), then Tukey's post hoc analysis, were performed to evaluate whether there were significant differences between the treatments and the control group. Using Origin 9.5, all of the graphs and histograms were created. LabVIEW (13.0.1f5) was used to capture all of the OCT image data, and MATLAB (R2016b) software was utilized to analyze the bOCT data that was gathered.

3. Results and discussion

3.1. Comparison between OCT and bOCT images

The OCT structural images and bOCT biospeckle contrast images of lentil seeds after 24 h of exposure to different treatments are compared to make sure the capability of monitoring internal biological activities as shown in Fig. 2 a-h with logarithmic intensity scale.

Fig. 2 a-d corresponds to OCT images. Fig. 2 e-h corresponds to bOCT images. The internal laminar structure of the seed can be seen in OCT structural pictures, where bright parts signify a strong reflectivity signal and dark regions signify a weak reflectivity signal. At the top of the structural image, the seed coat and epidermis are clearly visible due to their high reflectivity. However, any change of internal biological activity could not be examined using OCT images as compared to bOCT images. The bOCT images were obtained from a series of OCT frames acquired in a few seconds across the acquisition period under each treatment using Eq. (3). Red areas in the biospeckle images denote more temporal activity or fluctuation, while blue areas denote lower temporal activity or fluctuation. There are fewer red regions in both 100 mg L^{-1} Zn and MPs exposure compared to the control. However, in the combined treatment of MPs and Zn, red regions are higher than 100 mg L^{-1} Zn and MPs alone and fewer than control treatment which was not seen in the OCT structural images.

The change of optical reflectivity is measured by OCT and observed as structures. In addition to laminar organization, the OCT pictures contain tiny granular structures termed speckles that were created by the seed's mitochondria, Golgi bodies, and potentially its chloroplasts, which are smaller internal scattering microstructures. Cell development, cell division, and cytoplasmic flow may be responsible for the motions of these structures, and these movements would alter the biospeckles shown in the bOCT pictures. There was a noticeable decrease in biospeckle contrast for both individual effects of PEMPs and Zn. However, for the combined treatment of PEMPs and Zn, the contrast is higher than the individual treatments and lower than the control treatment. This distinct shift in contrast could only be seen in bOCT biospeckle pictures and not in OCT structural images.

3.2. Comparison of bOCT images with different treatments over a short duration

In this study, bOCT observations were taken over a short duration starting from 0 h (before exposure), 6 h, 12 h, and 24 h after exposure to different treatments and compared to observe the synergic effect of PEMPs and Zn. Results are shown in Fig. 3. A significant effect could be seen from bOCT images even after a relatively short imbibition time. The control samples for each observational time frame are shown in the first row of Fig. 3 a-d. A significant increment of red color density of the bOCT contrast images could be observed with increasing time. Hence, the internal biological activities have been enhanced with increasing time due to the activation of energy metabolism and water uptake's germination-induced cell growth. All of the treatments displayed the same tendency. However, the red color density is low for both PEMPs (Fig. 3 e-h) and Zn (Fig. 3 i-l) exposure compared to the control. Thus, a significant reduction of internal biological activities could be observed for both PEMPs and Zn exposure (Fig. 3 e-l). Interestingly, a significant increment of red color density was observed for the combined effect of PEMPs, and Zn compared to both PEMPs and Zn individual exposure (Fig. 3 m-p). This could be seen as a reduction of heavy metal bioavailability under the combined treatment owing to the adsorption of Zn by the PEMPs according to the literature [21].

3.3. Quantitative analysis and normalized bOCT contrast

A quantitative comparison of bOCT contrast images over each treatment is shown in Fig. 3. In order to obtain a reliable comparison between treatments, a qualitative analysis was performed with the help of the region of interest (ROI) (Fig. S1). The ROI is specific to local rectangular sections located close to the seed coat and used to calculate contrast qualitatively. The seed coat was considered when choosing the ROIs. as much as possible sincesiginificant changes are expected and thus significant activity due to external stimuli could be observed near the seed coat. Moreover, at the bottom of each bOCT image red color density is significantly high. This is due to the high noise level in the deepest region. Therefore, bOCT can used to scan up to few hundred micrometers depth accurately. Each bOCT
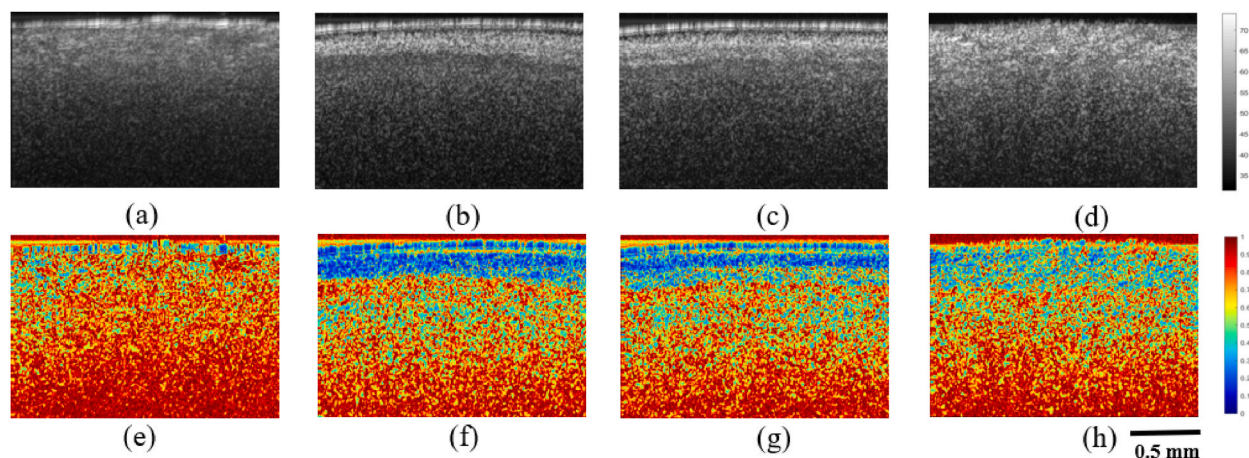

Fig. 2. OCT structural (uper row) and bOCT contrast images (lower row) after 24 h exposure of control (a, e), 100 mg L^{-1} MPs (b, f), 100 mg L^{-1} Zn (c, g), and MPs + Zn (d, h). There was a noticeable decrease in biospeckle contrast for both individual effects of PEMPs and Zn. However, for the combined treatment of PEMPs and Zn, the contrast is higher than the individual treatments and lower than the control treatment. This distinct shift in contrast could only be seen in bOCT biospeckle pictures and not in OCT structural images.
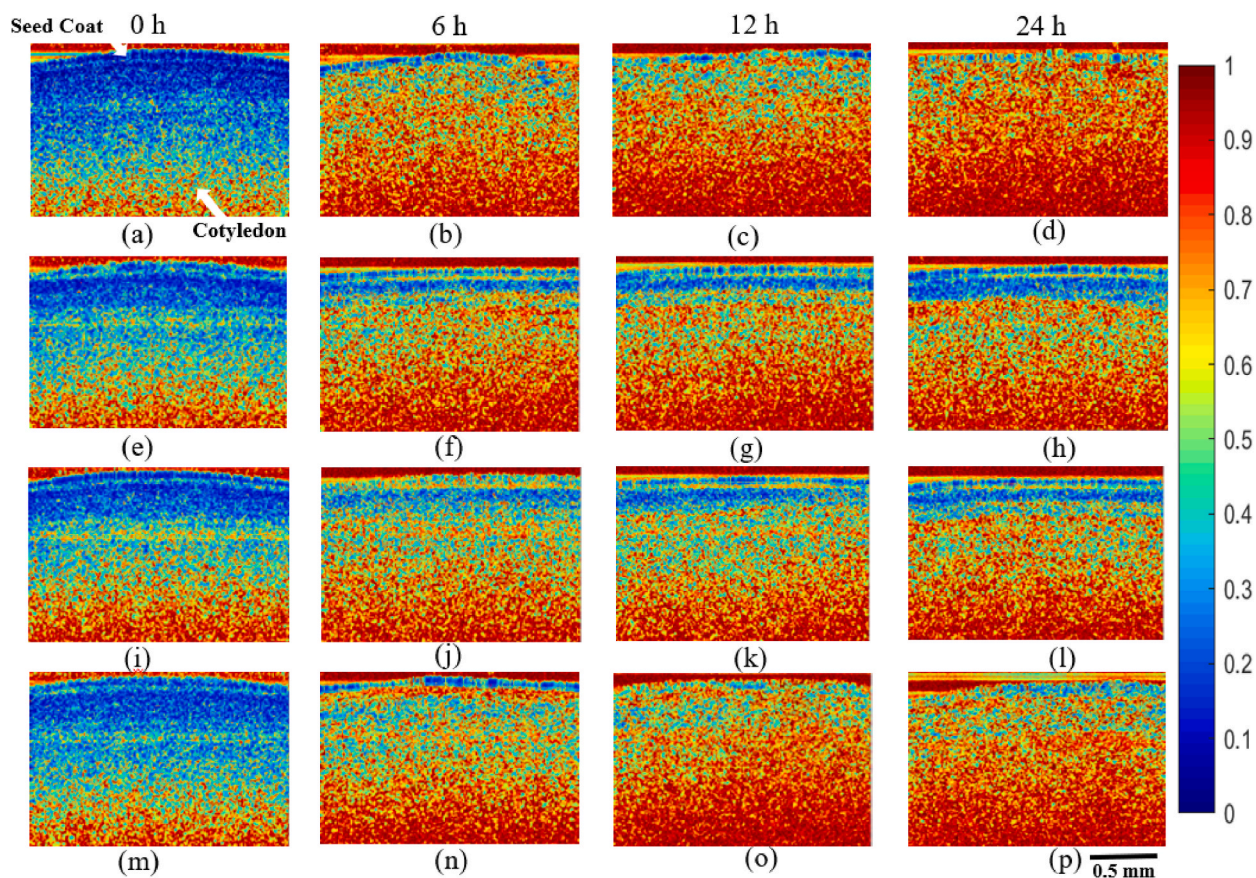
Fig. 3. Comparison of bOCT images at 0h, 6h, 12h, and 24h. Control samples (a)–(d); Samples treated with 100 mg L^{-1} MPs (e)–(h); Samples treated with 100 mg L^{-1} Zn (i)–(l); Samples treated with both 100 mg L^{-1} MPs and Zn (m)–(p). A clear reduction of biospeckle contrast could be seen for both individual effects of PEMPs and Zn. However, for the combined treatment of PEMPs and Zn, the contrast is higher than the individual treatments and lower than the control treatment. When concentration rises, the effect becomes more apparent.
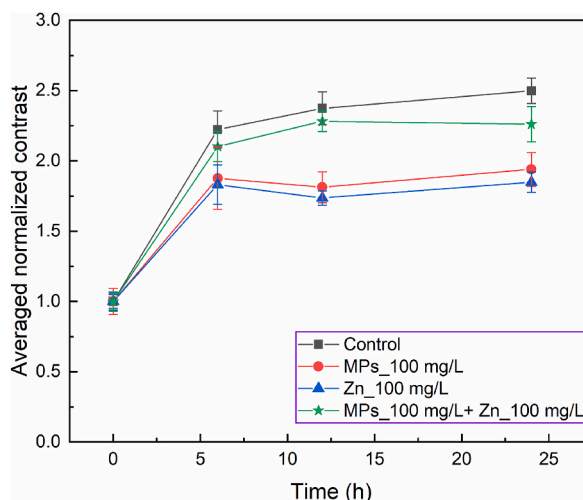

Fig. 4. Averaged normalized bOCT contrast of lentil seeds under control, PEMPs alone, Zn alone, PEMPs and Zn combined throughout a 24 h period. Due to the interaction between PEMPs and Zn, reductions in ANC might be seen for both individual exposure to PEMPs and Zn as well as for Zn toxicity when combined with PEMPs.

contrast image in this study had six ROIs chosen, and the average of those six local contrast values was calculated to create the average local contrast, or ALC. The overall average of contrast was then calculated by averaging six sets of ALC across the six seeds under the same treatment condition. It is a well-known fact that there is an individual variation between seeds. Therefore, to eliminate the individual variation among the seeds and treatments normalization process was used. First, the results obtained at 0 h or earlier than the imbibition condition were used to normalize the ALC of each treatment, and the result was referred to as normalized contrast (NC). The average normalized contrast (ANC) was then calculated by averaging six NCs across six seeds. The comparison of ANC across all treatments is shown in Fig. 4. For all of the observation time frames, it was possible to clearly identify substantial ANC decreases ($p <$ 0.05) for both PEMPs and Zn exposure in comparison to the control. For the PEMPs exposure, respective reduction rates compared to that of control are 15.6 %, 23.7 %, and 22.4 % at 6 h, 12 h, and 24 h respectively. The same pattern could be seen with Zn exposure, where the corresponding reduction rates from control are 17.6 %, 26.9 %, and 26 % at 6 h, 12 h, and 24 h, respectively. There is a marginal reduction of ANC of Zn exposure compared to MPs exposure. However, the reduction is not significant. For the combined effect the reduction of ANC could be seen with a respective reduction rate of 5.4 %, 3.9 %, and 9.5 % at 6 h, 12 h, and 24 h respectively where the significant effect could be observed only after 24 h of exposure. Interestingly, when comparing the PEMPs and Zn individual exposure with combined treatment, a significant increment of ANC could be observed where all the differences are significant except the difference at 6 h. This result clearly emphasizes the reduction of Zn toxicity when combined with PEMPs due to the interaction of MPs and Zn.

In this study, the concentration of PEMPs was selected from our previous studies, especially to induce an adverse effect on lentils [7]. It was found that both 100 mg L^{-1} PEMPs and 100 mg L^{-1} Zn have a significant adverse effect on lentil seed germination, and seedling growth. Numerous studies have documented how MPs negatively affect seed germination and plant growth [6,47]. The adverse effect is more significant when the concentration increases. However, the negative effect was seen in the majority of research studies when the concentration of PEMPs exceeded 100 mg L^{-1}. Thus, in this study also 100 mg L^{-1} was selected as the MPs concentration and the significant dicrement of biospeckle contrast was examined when compared to control after 12 h of exposure (Fig. 3 e-h and Fig. 4). Thus, the internal biological activity has been reduced for the exposure of 100 mg L^{-1} PEMPs. It is speculated that PEMPs could build up close to the seed coat and block the seed coat's pores, preventing water and nutrients from being absorbed, which would lead to the diminution of internal biological activity [5,6].

In general, lentil species have uneven seed coat surfaces covered with distinctive conical papillae [48]. Experimental observations revealed that the average lentil pore size could range from 4 to 8 μm [49]. The polyethylene microspheres used in this study have particle sizes ranging from 0.744 to 4.990 μm. Consequently, PEMPs may prevent the ingestion of nutrients and water through the physical blockage of pores of seed capsules, which would reduce internal activity. The bOCT results of the current research corroborate with the study performed by Refs. [5,6], and [25], where they confirmed the short-term, transient adverse effect of PEMPs on seed germination and seedling growth by confocal microscopy of fluorescent microplastics and traditional metrics like germination rate and viability, plant height, biomass, leaf area, relative root growth, and relative shoot growth.

The Zn concentration was also selected based on our previous study where 100 mg L^{-1} Zn induced a significant adverse effect [13]. It is a well-known fact that higher Zn concentrations (>50 mg L^{-1}) behave as a heavy metal inducing adverse effects in which the lower Zn concentrations behave as a micronutrient inducing a positive effect on plant growth. High quantities of heavy metals can severely impair seed germination and seedling growth by interfering with a variety of biochemical and physiological processes that harm cells, break down protein synthesis, and alter enzyme activity [50]. The effectiveness or ineffectiveness of germination is caused by a variety of enzyme activities. Gibberellic acid (GA3) and endogenous abscisic acid (ABA) are two of them that are crucial. According to literature, high Zn concentrations could increase ABA contents and decrease GA3 contents, which would reduce the germination of chickpea (*Cicer arietinum*) seeds [51]. Further, the presence of ABA can prevent the development of radicals and prevent germination, decreasing internal activity as a result [52]. Therefore, 100 mg L^{-1} Zn could reduce the internal biological activity of lentil seeds while reducing seed germination. This decrease in germination activity was tracked using a biospeckle contrast, and as can be shown in Fig. 3 i-l and Fig. 4, a substantial decrease was seen when compared to the control. Such a result is primarily consistent with previous studies [53].

Few studies describe the synergic effect of MPs and heavy metals on plant growth and seed germination. The reduction of heavy metal toxicity and bioavailability was observed when combining MPs with heavy metal [21,22] due to the adsorption ability of heavy metals on microplastics [14]. The adsorption isotherms were better described by the Langmuir model, which indicates the main mechanism as chemisorption [16]. The results of the present study are in line with previous studies where the increment of ANC was observed for the combined treatment compared to individual treatments as shown in Fig. 3 m-p and Fig. 4.

3.4. Comparison of bOCT results with conventional measures

Few traditional measurements, including germination viability, germination rate, seed vigor, shoot length, root length, seedlings' fresh and dried weight, and metal uptake studies, were carried out to compare and confirm the reliability of the acquired bOCT data after the exposure of four different treatments of control, 100 mg L^{-1} PEMPs alone, 100 mg L^{-1} Zn alone, and combined treatment of 100 mg L^{-1} PEMPs and 100 mg L^{-1} Zn.

3.4.1. Indexes of seed germination and growth of seedlings

For measuring the seed vigor and germination capacity of seeds in the face of various environmental stresses, the terms germination viability (GV) and germination rate (GR) are frequently used. The number of seeds from each treatment that had germinated after two days of exposure was counted in order to determine the germination viability (Eq. (4)), and following seven days of exposure, the final

germination rate was calculated in accordance with Eq. (5). Both 100 mg L^{-1} PEMPs (P < 0.05) and 100 mg L^{-1} Zn (P < 0.05) alone caused a significant reduction in germination viability (P 0.05) when compared to the control. The reduction of germination rate under combined treatment is not significant compared to the control. However, the increment of germination rate and germination viability could be seen for the combined treatment compared to MPs alone and Zn alone in which the significant increment was observed only for PEMPs alone treatment (Table 1). The same effect on lentil seed germination was observed from bOCT technique where a significant decrement of biospeckle contrast was observed just after 12 h of exposure before the germination. The observed results of GV and GR imply the reduction of Zn toxicity when combined with the PEMPs and Zn.

The same tendency could be seen for both average root length and shoot length as well. A significant reduction (P < 0.05) of average root and shoot length was observed for all the treatments compared to the control. However, compared to PEMPs alone and Zn alone, a significant increment (P < 0.05) of average root and shoot length was observed for the combined treatment. This is believed to be from the interaction of MPs and Zn in the aqueous solution.

3.4.2. The weight of lentil seedlings both wet and dry

There are different conventional measurements used to monitor the acute toxicity induced by the external stressor on plant growth. Seedling fresh weight (FW) and dry weight (DW) have been used frequently as crucial indicators among them [28]. In this study, the FW and DW of seedlings were monitored as shown in Fig. 5 to compare against acquired bOCT results. The root FW and DW showed a significant reduction (P < 0.01) for both 100 mg L^{-1} PEMPs and Zn alone compared to the control where the reduction for the combined treatments was not significant compared to the control. However, in comparison to 100 mg L^{-1} PEMPs and Zn individual treatments, the combined treatments have a significant increment (P < 0.01) of root FW and DW. Almost the same tendency could be seen for shoot FW and DW as well.

3.4.3. Comparison of seed vigor with biospeckle contrast

The seed vigor measurements were performed after 24 h of exposure to PEMPs and Zn as referred to section 2.5, to compare with the observed bOCT results because the 24 h estimate for the typical lentil germination time. The reduction of TTC to TPF occurs owing to the action of diverse dehydrogenases in the seeds, thus the degree of the seed vigor could be determined by measuring the absorbance of TPF [44]. The results of TPF absorbance of lentil seeds exposed to different treatments after 24 h of exposure are shown in Table 2. The absorbance of TPF of lentil seeds in MPs and Zn individual treatments decreased by 18.8 % and 29.5 % respectively compared to that of the control. However, the absorbance of lentil seeds in the combined treatments decreased by just 12.1 % compared to the control. When the reduction content of TTC is higher, the absorbance is also higher. Consequently, the greater the seed vigor. These results suggested that all the treatments impede the seed vigor compared to that of the control. However, a significant increment of lentil seed vigor in combined treatment could be observed compared to lentil seed vigor in the individual treatments of PEMPs and Zn. The amount of TTC that can be converted to TPF in the more metabolically active seeds increases with the average biospeckle contrast of the seeds with higher biological activity. The similar trend of the bOCT and TTC results may be explained by this. The findings suggest that bOCT may have been used to measure this metabolic activity.

3.5. Zn uptake analysis

The Zn uptake measurements were carried out for 7 days old seedlings as a comparison with the bOCT results since one of the main concerns in this study was the interaction of PEMPs and Zn and how it affects lentil seed germination and seedling growth. The bOCT results clearly emphasized that the toxicity of Zn was reduced for the combined treatments of 100 mg L^{-1} PEMPs and Zn. The reason could be the combined treatment may lower the amount of Zn uptake by the seedling owing to the interaction of PEMPs and Zn in an aqueous solution. Therefore, Zn uptakes of plants were measured using ICP-AES, and results are shown in Table 3 to make sure the exact amount of Zn uptake by the seedlings, especially in the combined treatment. During the experiment 0.01 % Hyponex solution was added to each Petry dish as a nutrient solution that contained a small amount of Zn. Therefore, Zn accumulation in the control treatment was observed as 25.35 mg/kg. In the PEMPs 100 mg L^{-1} individual treatment, the reduction of Zn accumulation (21.84 mg/kg) was examined compared to that of the control. This could be the reduction of Zn uptake due to the interaction of MPs and Zn in the nutrient solution. However, the reduction is not statistically significant. The Zn accumulation under 100 mg L^{-1} Zn individual treatment (946.21 mg/kg) is significantly higher than all other treatments which far exceeded the threshold. Therefore, lentil seedlings in 100 mg L^{-1} Zn showed a strong negative response. It is a well-known fact that Zn is a micronutrient, but in excess, it can pose a threat

Table 1

The effects of four different treatments (Control, 100 mg L^{-1} PEMPs alone, 100 mg L^{-1} Zn alone, and 100 mg L^{-1} MPs and Zn combined) on various conventional growth metrics, including seed germination rate, average root length, and shoot length in 7 days old lentil seedlings as well as germination viability in 2 days old lentil seedlings. Data reflects mean ± SD (n = 3). The different letters, a, b, and c, indicate statistical variations between treatments.

Treatments	Germination viability (GV) (%)	Germination rate (GR) (%)	Average root length (mm)	Average shoot length (mm)
Control	83.3 ± 8.33a	86.1 ± 4.81a	40.38 ± 1.14a	34.7 ± 2.17a
MPs_100 mg L^{-1}	36.1 ± 9.62c	47.2 ± 4.81b	16.45 ± 3.33c	16.76 ± 1.81c
Zn_100 mg L^{-1}	47.2 ± 4.81BCE	55.6 ± 4.81b	9.12 ± 0.54d	17.96 ± 1.28c
MPs_100 mg L^{-1} + Zn_100 mg L^{-1}	66.7 ± 23.05 ab	72.2 ± 12.73a	34.84 ± 0.64b	27.49 ± 2.99b
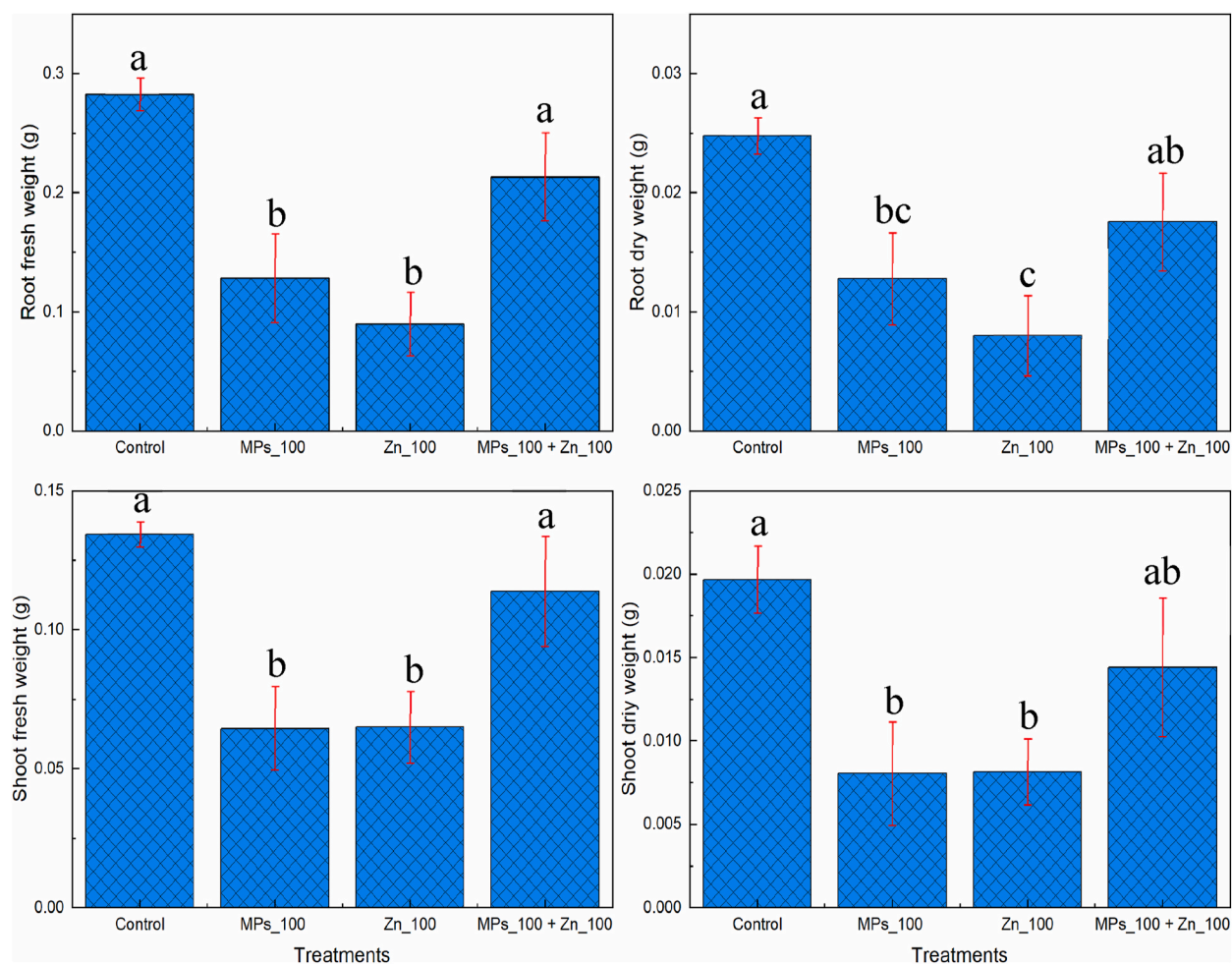
Fig. 5. Effects of different treatments (control, 100 mg L^{-1} Zn alone, 100 mg L^{-1} PEMPs alone, 100 mg L^{-1} Zn and PEMPs combined) on many standard growth metrics in seedlings of lentils that are seven days old, root fresh weight, root dry weight, shoot fresh weight, shoot dry weight. A significant reduction (P < 0.01) for both 100 mg L^{-1} PEMPs and Zn individual treatments was observed compared to control where a significant increment could be seen for combined treatment compared to individual treatments of PEMPs and Zn. Data reflect mean ± SD (n = 3). Different letters, a b c, represent statistical differences between treatments.

Table 2
TPF absorbance of seeds exposed to different treatments after 24 h of exposure. Data reflect mean ± SD (n = 3). Different letters, a b c, represent statistical differences between treatments. Different letters, a b c, represent statistical differences between treatments (p < 0.05; N = 3).

Treatments	Absorbance (485 nm)
Control	1.49 ± 0.080a
MPs_100 mg L^{-1}	1.21 ± 0.003b
Zn_100 mg L^{-1}	1.05 ± 0.030c
MPs_100 mg L^{-1} + Zn_100 mg L^{-1}	1.31 ± 0.001b

to plants [53]. Interestingly, the amount of Zn uptake was calculated as 383.79 mg/kg for combined treatment which was significantly lower than 100 mg L^{-1} Zn alone and significantly higher than 100 mg L^{-1} PEMPs alone treatments. Therefore, the amount of Zn uptake was significantly reduced by the combined treatment and diminished the Zn toxicity due to the interaction of MPs and Zn in an aqueous solution [14].

Furthermore, the bioavailability of heavy metals from wheat seedlings was decreased by copper and cadmium adsorption onto polystyrene microplastics as a result of chemisorption [21]. Furthermore, in Ref. [54], due to changes in soil parameters, such as sulphate and dissolved iron, polyvinyl chloride was found to reduce the bioavailability of methylmercury for paddy soils. These results

Table 3

The Zn uptake in 7 days old lentil seedlings. Data reflect mean $\pm$ SD (n = 3). Different letters, a b c, represent statistical differences between treatments. Different letters, a b c, represent statistical differences between treatments ($p <$ 0.05; N = 3).

Treatments	Zn uptake (mg/kg)
Control	$25.35 \pm 3.55c$
MPs_100 mg L^{-1}	$21.84 \pm 2.54c$
Zn_100 mg L^{-1}	$946.21 \pm 81.33a$
MPs_100 mg L^{-1} + Zn_100 mg L^{-1}	$383.79 \pm 29.75b$

are in line with the results of the present study where the reduction of bioavailability was observed due to the interaction of MPs and heavy metal in aqueous solution through chemisorption. However, there are some studies that reported the increment of metal uptake for combined treatment inducing significant adverse effects [55,56]. It has been reported that plants can accumulate heavy metals through their adsorption onto the root surface in soil–plant systems [57]; therefore, the factors influencing metal adsorption onto the root surface may affect the accumulation of heavy metals in vegetables. To examine the combined impacts of PEMPs, Zn, and Cd on soil qualities and lettuce development, a pot experiment was conducted [30]. A similar effect was observed emphasizing the increment of heavy metal bioavailability under the combined exposure of both metals. The presence of microplastics in the extensively contaminated agricultural soil elevated the readily available Zn concentration more than the harmful Cd concentration. Moreover, the effect of polylactic acid (PLA) microplastics and lead (Pb^{2+}) on the growth and physiological characteristics of buckwheat was investigated [31]. The results imply that both PLA-MPs and Pb^{2+} inhibited Tartary buckwheat growth. However, PLA-MPs combined treatment adsorbed Pb^{2+} by chemisorption but did not increase or reduce the toxicity of Pb^{2+} at the macroscopic level.

In this study, the acute toxicity effect of PEMPs and Zn on lentil seed germination and seedling growth was observed with the help of bOCT technology. Therefore, long-term investigations should be performed in field conditions to understand the influence of heavy metals on microplastics and their natural biodegradability in soil-plant systems. The potential impacts on soil health and microbial communities due to synergic effect of MPs and heavy metals need to be investigated. The combined effects of heavy metals and microplastics on ecosystems and human health must thus be explored through future research. Hence, further studies should be carried out to comprehensively assess the synergic effect of MPs and heavy metals in both aquatic and terrestrial ecosystems considering the impact on plants, soil, microbial communities and human health.

4. Conclusions

The current work highlights the capability of bOCT to quickly detect the synergistic effects of PEMPs and Zn on lentil seed germination within a few hours of treatment. There are studies describing the combined effect of MPs and heavy metals, however, according to our knowledge, there are no investigations that have been done to observe how seeds' internal biological activities change when exposed to MPs and Zn together reasonably early before germination. Interestingly, within 12 h of exposure to all treatments in this investigation, significant impact on lentil seed germination was seen. A significant reduction of internal biological activity was observed for both PEMPs and Zn individual treatments. On the contrary, for the combined treatment, a significant increment of internal biological activity was observed compared to both individual treatments of PEMPs and Zn. In addition, a similar decline in biological activity was seen in contrast to the control group as well. For comparison, conventional measures of seed vigor, germination viability, germination rate, root and shoot length, root and shoot FW, root and shoot DW, and Zn uptake analyses were also assessed. The results were consistent with those of the bOCT. However, it should be pointed out that the conventional measurements took a minimum of 2 days to exhibit a significant effect in which the same effect was observed within 12 h of exposure from bOCT. These results implied that the combination of PEMPs and Zn significantly reduced the accumulation of Zn in lentil seedlings while reducing the toxic effects of heavy metals on lentils due to the interaction of heavy metals and PEMPs in an aqueous solution. Further research is needed to elucidate the underlying mechanism by which temporal dynamics speckles can unveil the synergistic impact of microplastics (MPs) and heavy metals on both seed germination and seedling growth.

CRediT authorship contribution statement

Y. Sanath K. De Silva: Data curation, Formal analysis, Investigation, Methodology, Validation, Writing – original draft, Data curation, Formal analysis, Investigation, Methodology, Validation, Writing – original draft. **Uma Maheswari Rajagopalan:** Conceptualization, Funding acquisition, Investigation, Methodology, Supervision, Writing – review & editing. **Hirofumi Kadono:** Conceptualization, Funding acquisition, Investigation, Software, Supervision, Writing – review & editing. **Danyang Li:** Data curation.

Declaration of competing interest

The authors declare that they have no known competing financial interests or personal relationships that could have appeared to influence the work reported in this paper.

Acknowledgments

Appendix A. Supplementary data

Supplementary data to this article can be found online at https://doi.org/10.1016/j.heliyon.2023.e21464.

References

[1] M. Cole, P. Lindeque, C. Halsband, T.S. Galloway, Microplastics as contaminants in the marine environment: a review, Mar. Pollut. Bull. 62 (2011) 2588–2597, https://doi.org/10.1016/j.marpolbul.2011.09.025.
[2] H.A. Nel, P.W. Froneman, A quantitative analysis of microplastic pollution along the south-eastern coastline of South Africa, Mar. Pollut. Bull. 101 (2015) 274–279, https://doi.org/10.1016/j.marpolbul.2015.09.043.
[3] A.L. Andrady, Microplastics in the marine environment, Mar. Pollut. Bull. 62 (2011) 1596–1605, https://doi.org/10.1016/j.marpolbul.2011.05.030.
[4] Y.S.K. De Silva, U.M. Rajagopalan, H. Kadono, Microplastics on the growth of plants and seed germination in aquatic and terrestrial ecosystems, Glob. J. Environ. Sci. Manag. 7 (2021) 1–22, https://doi.org/10.22034/gjesm.2021.03.03.
[5] M.A. Urbina, F. Correa, F. Aburto, J.P. Ferrio, Adsorption of polyethylene microbeads and physiological effects on hydroponic maize, Sci. Total Environ. 741 (2020), 140216, https://doi.org/10.1016/j.scitotenv.2020.140216.
[6] T. Bosker, L.J. Bouwman, N.R. Brun, P. Behrens, M.G. Vijver, Microplastics accumulate on pores in seed capsule and delay germination and root growth of the terrestrial vascular plant Lepidium sativum, Chemosphere 226 (2019) 774–781, https://doi.org/10.1016/j.chemosphere.2019.03.163.
[7] Y.S.K. De Silva, U.M. Rajagopalan, H. Kadono, D. Li, Effects of microplastics on lentil (Lens culinaris) seed germination and seedling growth, Chemosphere 303 (2022), 135162, https://doi.org/10.1016/j.chemosphere.2022.135162.
[8] Y.S.K. De Silva, U.M. Rajagopalan, D. Li, H. Kadono, Optical screening method to observe the biological activities of lentil (Lens culinaris) seeds quantitatively under the exposure of polyethylene microplastics (PEMPs) using ultrahigh accurate biospeckle optical coherence tomography, SPIE (2022) 19, https://doi.org/10.1117/12.2620176.
[9] Z. Hassan, M.G.M. Aarts, Opportunities and feasibilities for biotechnological improvement of Zn, Cd or Ni tolerance and accumulation in plants, Environ. Exp. Bot. 72 (2011) 53–63, https://doi.org/10.1016/j.envexpbot.2010.04.003.
[10] S. Gautam, Effects of zinc supply on its uptake, growth and biochemical constituents in lentil, Indian J. Plant Physiol. 14 (2009) 67–70.
[11] K.V.S.K. Prasad, P.P. Saradhi, P. Sharmila, Concerted action of antioxidant enzymes and curtailed growth under zinc toxicity in Brassica juncea, Environ. Exp. Bot. 42 (1999) 243, https://doi.org/10.1016/s0098-8472(99)00045-3.
[12] D. Liu, et al., Effect of Zn toxicity on root morphology, ultrastructure, and the ability to accumulate Zn in Moso bamboo (Phyllostachys pubescens), Environ. Sci. Pollut. Res. 21 (2014) 13615–13624, https://doi.org/10.1007/s11356-014-3271-3.
[13] Y.S.K. De Silva, U.M. Rajagopalan, H. Kadono, D. Li, Positive and negative phenotyping of increasing Zn concentrations by Biospeckle Optical Coherence Tomography in speedy monitoring on lentil (Lens culinaris) seed germination and seedling growth, Plant Stress 2 (2021), 100041, https://doi.org/10.1016/j.stress.2021.100041.
[14] Q. Wang, Y. Zhang, X. Wangjin, Y. Wang, G. Meng, Y. Chen, The adsorption behavior of metals in aqueous solution by microplastics effected by UV radiation, J. Environ. Sci. 87 (2020) 272–280, https://doi.org/10.1016/j.jes.2019.07.006.
[15] Q. Zhou, et al., Total concentrations and sources of heavy metal pollution in global river and lake water bodies from 1972 to 2017, Glob. Ecol. Conserv. (2020) 22, https://doi.org/10.1016/j.gecco.2020.e00925.
[16] V. Godoy, G. Blázquez, M. Calero, L. Quesada, M.A. Martín-Lara, The potential of microplastics as carriers of metals, Environ. Pollut. 255 (2019), https://doi.org/10.1016/j.envpol.2019.113363.
[17] Z. Lin, Y. Hu, Y. Yuan, B. Hu, B. Wang, Comparative analysis of kinetics and mechanisms for Pb(II) sorption onto three kinds of microplastics, Ecotoxicol. Environ. Saf. 208 (2021), https://doi.org/10.1016/j.ecoenv.2020.111451.
[18] A. Rizvi, A. Zaidi, F. Ameen, B. Ahmed, M.D.F. Alkahtani, M.S. Khan, Heavy metal induced stress on wheat: phytotoxicity and microbiological management, RSC Adv. 10 (2020) 38379–38403, https://doi.org/10.1039/d0ra05610c.
[19] A. Rizvi, et al., Maize associated bacterial microbiome linked mitigation of heavy metal stress: a multidimensional detoxification approach, Environ. Exp. Bot. 200 (2022), https://doi.org/10.1016/j.envexpbot.2022.104911.
[20] J. Park, et al., First evidence for mechanism of inverse ripening from in-situ TEM and phase-field study of δ′ precipitation in an Al-Li alloy, Sci. Rep. 9 (2019), https://doi.org/10.1038/s41598-019-40685-5.
[21] X. Zong, et al., Effects of polystyrene microplastic on uptake and toxicity of copper and cadmium in hydroponic wheat seedlings (Triticum aestivum L.), Ecotoxicol. Environ. Saf. 217 (2021), https://doi.org/10.1016/j.ecoenv.2021.112217.
[22] F. Wang, X. Zhang, S. Zhang, S. Zhang, C.A. Adams, Y. Sun, Effects of Co-contamination of microplastics and Cd on plant growth and Cd accumulation, Toxics 8 (2020) 1–12, https://doi.org/10.3390/TOXICS8020036.
[23] F. Wang, X. Zhang, S. Zhang, S. Zhang, Y. Sun, Interactions of microplastics and cadmium on plant growth and arbuscular mycorrhizal fungal communities in an agricultural soil, Chemosphere (2020) 254, https://doi.org/10.1016/j.chemosphere.2020.126791.
[24] Y. Liu, et al., Effects of microplastics on cadmium accumulation by rice and arbuscular mycorrhizal fungal communities in cadmium-contaminated soil, J. Hazard Mater. 442 (2023), https://doi.org/10.1016/j.jhazmat.2022.130102.
[25] B. Li, et al., Effects of plastic particles on germination and growth of soybean (Glycine max): a pot experiment under field condition, Environ. Pollut. 272 (2021), 116418, https://doi.org/10.1016/j.envpol.2020.116418.
[26] J. Li, et al., Micro-polyethylene particles reduce the toxicity of nano zinc oxide in marine microalgae by adsorption, Environ. Pollut. 290 (2021), 118042, https://doi.org/10.1016/j.envpol.2021.118042.
[27] F. Wang, X. Feng, Y. Liu, C.A. Adams, Y. Sun, S. Zhang, Micro(nano)plastics and terrestrial plants: up-to-date knowledge on uptake, translocation, and phytotoxicity, Resour. Conserv. Recycl. 185 (2022), https://doi.org/10.1016/j.resconrec.2022.106503.
[28] M.Z. Alam, M.A. Hoque, G.J. Ahammed, R. McGee, L. Carpenter-Boggs, Arsenic accumulation in lentil (Lens culinaris) genotypes and risk associated with the consumption of grains, Sci. Rep. 9 (2019) 1–9, https://doi.org/10.1038/s41598-019-45855-z.
[29] M.S. Hossain, et al., Insights into acetate-mediated copper homeostasis and antioxidant defense in lentil under excessive copper stress, Environ. Pollut. 258 (2020), 113544, https://doi.org/10.1016/j.envpol.2019.113544.
[30] J. Bethanis, E.E. Golia, Revealing the combined effects of microplastics, Zn, and Cd on soil properties and metal accumulation by leafy vegetables: a preliminary investigation by a laboratory experiment, Soil. Syst. 7 (2023) 65, https://doi.org/10.3390/soilsystems7030065.
[31] X. Tian, et al., Effect of polylactic acid microplastics and lead on the growth and physiological characteristics of buckwheat, Chemosphere 337 (2023), 139356, https://doi.org/10.1016/j.chemosphere.2023.139356.

[32] D. Huang, E.A. Swanson, C.P. Lin, J.S. Schuman, W.G. Stinson, W. Chang, M.R. Hee, T. Flotire, K. Gregory, C. Puliafito, J.G. Fujimoto, Optical Coherence 1–4 (1991).

[33] A. Davis, O. Levecq, H. Azimani, D. Siret, A. Dubois, Simultaneous dual-band line-field confocal optical coherence tomography: application to skin imaging, Biomed. Opt Express 10 (2019) 694, https://doi.org/10.1364/boe.10.000694.

[34] R.E. Wijesinghe, et al., Optical screening of Venturianashicola caused Pyruspyrifolia (Asian pear) scab using optical coherence tomography, Int. J. Appl. Eng. Res. 11 (2016) 7728–7731.

[35] A. Rateria, M. Mohan, K. Mukhopadhyay, R. Poddar, Investigation of Puccinia triticina contagion on wheat leaves using swept source optical coherence tomography, Optik 178 (2019) 932–937, https://doi.org/10.1016/j.ijleo.2018.10.005.

[36] L.K.T. Srimal, H. Kadono, U.M. Rajagopalan, Optical coherence tomography biospeckle imaging for fast monitoring varying surface responses of a plant leaf under ozone stress, Sensing Technologies for Biomaterial 8881 (2013) 88810H, https://doi.org/10.1117/12.2031062.

[37] L.K.T. Srimal, U.M. Rajagopalan, H. Kadono, Functional optical coherence tomography (fOCT) biospeckle imaging to investigate response of plant leaves to ultra-short term exposure of Ozone, J. Phys. Conf. Ser. 605 (2015), https://doi.org/10.1088/1742-6596/605/1/012013.

[38] U.M. Rajagopalan, M. Kabir, Y. Lim, H. Kadono, Biospeckle optical coherence tomography in speedy visualizing effects of foliar application of plant growth hormone to Chinese chives leaves, BMC Res. Notes 13 (2020) 1–6, https://doi.org/10.1186/s13104-020-05219-7.

[39] Y. Lim, K. Funada, H. Kadono, Monitor Biological Activities in Seed Germination by Biospeckle Optical Coherence Tomography, 2019, p. 9, https://doi.org/10.1117/12.2509725.

[40] D. Li, U.M. Rajagopalan, Y.S.K. De Silva, F. Liu, H. Kadono, Biospeckle optical coherence tomography (bOCT) in the speedy assessment of the responses of the seeds of raphanus sativus L . (kaiware daikon) to acid mine drainage (AMD), Appl. Sci. 12 (1) (2022) 355, https://doi.org/10.3390/app12010355.

[41] D. Li, U.M. Rajagopalan, H. Kadono, Y.S.K. De Silva, Biospeckle Optical Coherence Tomography (bOCT) reveals variable effects of acid mine drainage (AMD) on monocot and dicot seed germination, SPIE (2022) 20, https://doi.org/10.1117/12.2621440.

[42] D. Li, U.M. Rajagopalan, H. Kadono, Y.S.K. De Silva, A real-time, non-invasive technique for visualizing the effects of acid mine drainage (AMD) on soybean, Minerals 12 (2022) 1–12, https://doi.org/10.3390/min12101194.

[43] Y. Aizu, T. Asakura, Bio-speckle, in: A. Consortini (Ed.), Trends in Optics. Research, Development and Applications, Academic Press, San Diego, 1996, pp. 27–49.

[44] L. Lopez Del Egido, D. Navarro-Miró, V. Martinez-Heredia, P.E. Toorop, P.P.M. Iannetta, A spectrophotometric assay for robust viability testing of seed batches using 2,3,5-triphenyl tetrazolium chloride: using Hordeum vulgare L. as a model, Front. Plant Sci. 8 (2017), https://doi.org/10.3389/fpls.2017.00747.

[45] J. Liu, Z. Wei, J. Li, Effects of copper on leaf membrane structure and root activity of maize seedling, Bot. Stud. 55 (2014) 1–6, https://doi.org/10.1186/s40529-014-0047-5.

[46] Turk, et al., Seedling growth of three lentil cultivars under moisture stress, Asian J. Plant Sci. 3 (3) (2004) 394–397.

[47] X. Jiang, H. Chen, Y. Liao, Z. Ye, M. Li, G. Klobučar, Ecotoxicity and genotoxicity of polystyrene microplastics on higher plant Vicia faba, Environ. Pollut. 250 (2019) 831–838, https://doi.org/10.1016/j.envpol.2019.04.055.

[48] J.S. Hughes, B.G. Swanson, C. Hall, Microstructure of Lentil Seeds (Lens Culinaris) Follow This and Additional Works at, Recommended Citation, 1986, p. 5. https://digitalcommons.usu.edu/foodmicrostructure.

[49] F. Aouaini, S. Knani, M. Ben Yahia, A. Ben Lamine, Statistical physics studies of multilayer adsorption isotherm in food materials and pore size distribution, Phys. Stat. Mech. Appl. 432 (2015) 373–390, https://doi.org/10.1016/j.physa.2015.03.052.

[50] M. Seneviratne, N. Rajakaruna, M. Rizwan, H.M.S.P. Madawala, Y.S. Ok, M. Vithanage, Heavy metal-induced oxidative stress on seed germination and seedling development: a critical review, Environ. Geochem. Health 41 (2019) 1813–1831, https://doi.org/10.1007/s10653-017-0005-8.

[51] Ö. Atici, G. Ağar, P. Battal, Changes in phytohormone contents in chickpea seeds germinating under lead or zinc stress, Biol. Plant. (Prague) 49 (2005) 215–222, https://doi.org/10.1007/s10535-005-5222-9.

[52] H. Nonogaki, Seed germination - the biochemical and molecular mechanisms, Breed Sci. 56 (2006) 93–105, https://doi.org/10.1270/jsbbs.56.93.

[53] R. Nanda, V. Agrawal, Elucidation of zinc and copper induced oxidative stress, DNA damage and activation of defence system during seed germination in Cassia angustifolia Vahl, Environ. Exp. Bot. 125 (2016) 31–41, https://doi.org/10.1016/j.envexpbot.2016.02.001.

[54] X. Yang, et al., Microplastics influence on Hg methylation in diverse paddy soils, J. Hazard Mater. 423 (2022), https://doi.org/10.1016/j.jhazmat.2021.126895.

[55] A. Pinto-Poblete, J. Retamal-Salgado, M.D. López, N. Zapata, A. Sierra-Almeida, M. Schoebitz, Combined effect of microplastics and Cd alters the enzymatic activity of soil and the productivity of strawberry plants, Plants 11 (2022), https://doi.org/10.3390/plants11040536.

[56] H. Jia, D. Wu, Y. Yu, S. Han, L. Sun, M. Li, Impact of microplastics on bioaccumulation of heavy metals in rape (Brassica napus L.), Chemosphere (2022) 288, https://doi.org/10.1016/j.chemosphere.2021.132576.

[57] F. Wang, X. Wang, N. Song, Polyethylene microplastics increase cadmium uptake in lettuce (Lactuca sativa L.) by altering the soil microenvironment, Sci. Total Environ. (2021) 784, https://doi.org/10.1016/j.scitotenv.2021.147133.